ACS OMEGA

http://pubs.acs.org/journal/acsodf

Article

Transition Metal Layer Substitution in Mo_2CS_2 MXene for Improving Li Ion Surface Kinetics

Konstantina A. Papadopoulou and Stavros-Richard G. Christopoulos*

Cite This: https://doi.org/10.1021/acsomega.3c02080

Read Online

ACCESS | Metrics & More | Article Recommendations

ABSTRACT: We study the adsorption and mobility of a Li ion on the surface of the Mo_2CS_2 MXene by means of Density Functional Theory. We find that by substituting the Mo atoms of the upper MXene layer with V the mobility of the Li ion can be improved up to 95% while the material retains its metallic character. This fact indicates that $MoVCS_2$ is a promising candidate for anode electrode in Li-ion batteries, where the materials need to be conductive and the Li ion needs to have a small migration barrier.

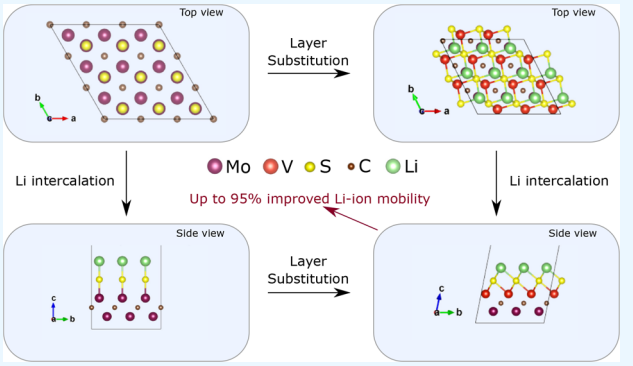

INTRODUCTION

The tunable properties[1−5] via control of the surface termination atoms of two-dimensional (2D) materials has made the latter the new point of interest regarding their use as anode materials in Li-ion batteries. Since 2011, a new ceramic material belongs in the 2D class, the MXenes. MXenes have the general formula $M_{n+1}X_nT_x$, (n = 1, 2, 3), with T a surface termination atom[2] and M an early transition metal. X stands for either carbon (C) or nitrogen (N).[4,6−9]

The most studied MXene is titanium carbide, Ti_3C_2,[10−17] which was also the first to be discovered[4,18] in 2011. Since then, zirconium carbide, Zr_2C, has garnered attention[5,19−22] after it was experimentally synthesized[20] by etching Al_3C_3 from layered $Zr_3Al_3C_5$ structures. However, the studies of Zr_2C as an anode electrode in ion batteries have been limited to O, OH, F, and S surface termination atoms, while a more extensive study of its use as an anode electrode in Li and non-Li ion batteries was conducted by Papadopoulou et al. in 2022.[5]

A year earlier than the synthesis of Zr_2C, in 2015, another MXene, molybdenum carbide, Mo_2C, was experimentally synthesized from the gallium-based atomic laminate Mo_2Ga_2C.[23] Band structure calculations have showed that Mo_2C is metallic when it is terminated by O or OH atoms, while it becomes semiconducting when it is terminated by F or Cl atoms.[23] The need to find new electrode materials with large ion capacities and fast charging rates has led to the question of whether Mo_2C can be used to enhance electrode performance.

In 2016, Sun et al.[24] theoretically verified that the bare and terminated Mo_2C is dynamically stable, a crucial property for an electrode. Also in 2016, Çakır et al.[25] theoretically studied the adsorption and diffusion of Li, Na, K, and Ca atoms on the surface of the Mo_2C MXene. They predicted that all the aforementioned atoms are strongly adsorbed on the surface of the monolayer MXene and found energy barriers for diffusions as low as 15 meV (K case).

In 2017, Mehta et al.[26] studied the adsorption of a Li ion on the Mo_2C monolayer doped with N and Mn using first-principles calculations. In particular, they (a) substituted one Mo atom from the upper MXene layer with Mn and (b) substituted a C atom with N. They found that the presence of the dopant atoms increases the Li adsorption and, thus, the ion storage capacity. However, there was no investigation regarding the mobility of the Li ion.

Finally, Mehta et al.[27] in 2019 performed first-principles calculations in S-terminated Mo_2C. They found that the Li ion has a diffusion barrier equal to 0.22 eV.

In the present work, we study a Li ion's adsorption and diffusion in the Mo_2CS_2 structure where the upper Mo MXene layer has been entirely substituted by vanadium, V. We denote this structure as $MoVCS_2$. We chose the S-terminated Mo_2CS_2 because previous studies[5,28,29] have shown that S lowers the migration barrier of the Li ion. The significance of this study

Received: March 28, 2023
Accepted: May 31, 2023

and the findings therein are 2-fold: First, we identify that the transition layer substitution results in a more stable material than the original configuration, a fact that opens the way for experimental work on MXenes with two different transition metals. Second, the very low Li-ion diffusion barriers calculated herein indicate the suitability of the aforementioned kind of MXenes for electrodes in Li-ion batteries.

COMPUTATIONAL METHODS

For the bulk structure of the bare Mo_2C, we used a starting structure typical of that found in theoretical analysis.[30] We performed Density Functional Theory (DFT) calculations as implemented in the CASTEP package[31−35] to derive the Mo_2CS_2 structure, where we randomly placed the S atom on top of the Mo atom, at a distance smaller than the bond length R_0[39] between the S and Mo which is equal to 2.33 Å.[40] DFT uses pseudopotentials[36] generated on the fly for the electron−ion interactions.[37] The exchange-correlation interactions between electrons were described using the corrected density functional of Perdew, Burke, and Ernzerhof (PBE) within the generalized gradient approximation (GGA).

A vacuum space of 30 Å was introduced to minimize the mirror interactions between adjacent MXene layers. A plane wave cutoff energy E_{cut} = 650 eV and a k-point spacing of 7 × 7 × 1 was used to converge the overall energy per formula unit to 0.5 × 10^{-5} eV. The structures were optimized using the BFGS geometry optimization method[35,38] and relaxed until the residual forces on the atoms were less than 0.01 eV × $Å^{-1}$. DFT produced a final structure where the interlayer distance between S and Mo increased by 28.3% from the one we had originally considered, while the interlayer distance between the two Mo layers decreased by 1.4%.

For the structures including the Li-ion, DFT was applied again after we inserted a single ion on the surface of Mo_2CS_2 at a distance from the S atom smaller than the bond length R_0[39] between the S and Li which is equal to 1.46 Å.[40]

For the adsorption energy, E_{ads}, for the Li ion on the Mo_2CS_2 surface, we used the following equation

$$E_{ads} = E_{Mo_2CS_2-Li} - E_{Mo_2CS_2} - E_{Reference} \quad (1)$$

where $E_{Reference}$ is the total energy of a single Li atom in the metal phase, $E_{Mo_2CS_2-Li}$ is the total energy of the structure including Li, and $E_{Mo_2CS_2}$ is the total energy of Mo_2CS_2 without the added ion.

Respectively, for the adsorption energy for the Li ion on the $MoVCS_2$ surface, we used the following equation

$$E_{ads} = E_{MoVCS_2-Li} - E_{MoVCS_2} - E_{Reference} \quad (2)$$

where E_{MoVCS_2-Li} is the total energy of the structure where the upper Mo layer has been substituted by V including the Li ion and E_{MoVCS_2} is the total energy of $MoVCS_2$ without the added ion.

In order to calculate the energy barrier for diffusion, E_{bar}, for the Li ion on each structure's surface, first we created a 2 × 1 × 1 supercell of each structure. The initial (reactant) position of the Li ion was the one predicted by the DFT calculations, while the final (product) position was the same position in the adjacent cell. We then applied an LST/QST transition state (TS) search algorithm in CASTEP.[41] The E_{bar} was calculated as the barrier from the initial position.

Finally, in order to calculate the Density of States (DOS) and thus characterize each material regarding its conductivity, we used the OPTADOS code[42] as implemented in CASTEP. For convenience, the Fermi level was shifted at 0 eV.

RESULTS AND DISCUSSION

The structure of the Mo_2CS_2 MXene is shown in Figure 1. The S atom sits directly above the Mo atom of the upper MXene layer. Furthermore, in Figure 2 we can see the structure of the $MoVCS_2$ where the upper Mo layer of Mo_2CS_2 has been substituted by V. This time, the termination atom S sits above a bottom layer Mo atom. The upper and bottom MXene layers are denoted as L1 and L2 in Figure 2.

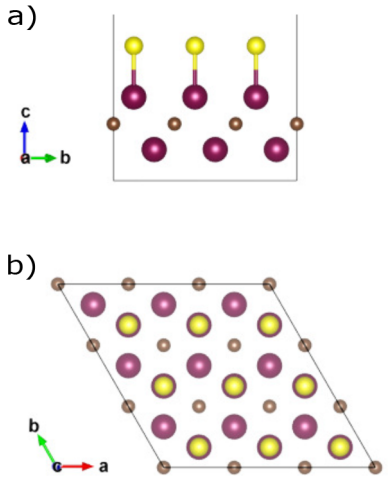

Figure 1. 3 × 3 × 1 supercell for the Mo_2CS_2 MXene layer after geometry optimization: (a) front view, (b) top view. Purple spheres: Mo atoms. Brown spheres: C atoms. Yellow spheres: S atoms.

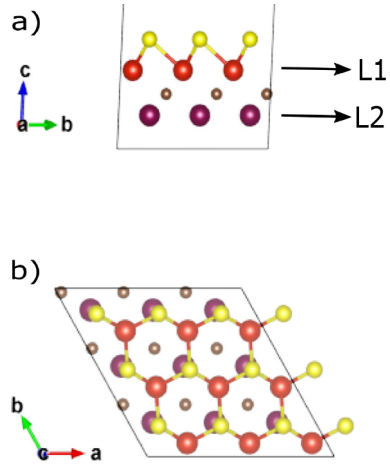

Figure 2. 3 × 3 × 1 supercell for the $MoVCS_2$ MXene layer after geometry optimization: (a) front view, (b) top view. Purple spheres: Mo atoms. Orange spheres: V atoms. Brown spheres: C atoms. Yellow spheres: S atoms.

The coordination number of the S atom is also different. In Mo_2CS_2 S bonds with only one atom belonging in L1, and in $MoVCS_2$ S bonds with three L1 atoms. Finally, the $MoVCS_2$ structure has 3.25% lower final energy than the Mo_2CS_2 one, a fact that indicates that it is also stable.

https://doi.org/10.1021/acsomega.3c02080
ACS Omega XXXX, XXX, XXX−XXX

As a next step, we added the Li ion on the surface of the two structures. In Figure 3 we see the Mo_2CS_2 case where the Li

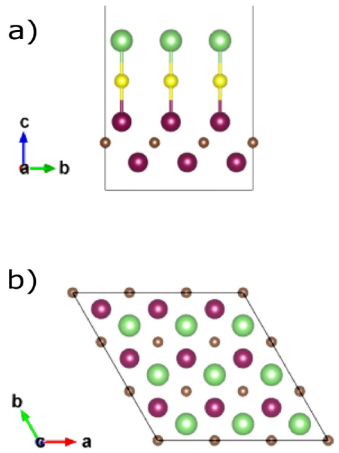

Figure 3. 3 × 3 × 1 supercell for the Mo_2CS_2 MXene layer after geometry optimization: (a) front view, (b) top view. Purple spheres: Mo atoms. Brown spheres: C atoms. Yellow spheres: S atoms. Green spheres: Li ions.

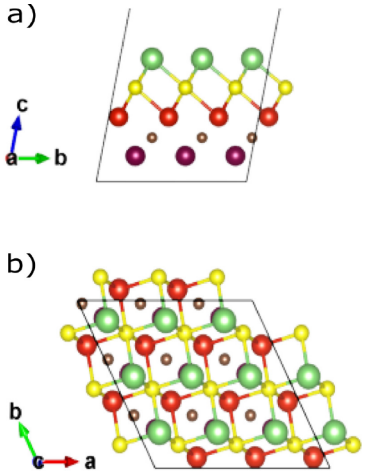

Figure 4. 3 × 3 × 1 supercell for the $MoVCS_2$ MXene layer after geometry optimization: (a) front view, (b) top view. Purple spheres: Mo atoms. Orange spheres: V atoms. Brown spheres: C atoms. Yellow spheres: S atoms. Green spheres: Li ions.

ion sits on top of the S termination, while in Figure 4 we see the $MoVCS_2$ case where the Li ion sits on top of a Mo atom of L2. In the latter case, the S termination atoms have slightly moved due to the bonds with Li and now sit above empty space. The $MoVCS_2$–Li structure also has 3.1% lower final energy than the Mo_2CS_2–Li one, a fact that indicates its stability.

The adsorption energies for the Li ion on each structure's surface are shown in Table 1. On Mo_2CS_2, Li appears to be more strongly adsorbed despite its smaller coordination number as described above. As Papadopoulou et al.[9] have showed, E_{ads} depends on the average distance between the termination atoms, the Li ions, and the L1 atoms. In fact, the smaller these distances are, the stronger the adsorption. Our results here are fully in support of this observation, as the

Table 1. Ion Adsorption Energies E_{ads} and the Migration Barrier Energies E_{bar}

Structure	E_{ads} (eV)	E_{bar} (eV)
Mo_2CS_2	−0.875	0.59
$MoVCS_2$	−0.784	0.03

distances between the aforementioned atoms in Mo_2CS_2 are smaller, on average, than in $MoVCS_2$ as indicated in Table 2.

Table 2. Average Distances between Atoms in Mo_2CS_2 (L1 = Mo) and $MoVCS_2$ (L1 = V)

Atoms	Mo_2CS_2 (Å)	$MoVCS_2$ (Å)
L1–S	2.235	2.405
S–Li	2.205	2.387

Also in Table 1, we can see the migration barriers E_{bar} for the Li ion. One can see that the substitution of Mo with V lowers the energy barrier by 95% (0.59 eV in Mo_2CS_2 vs 0.03 eV in $MoVCS_2$). This fact is significant since we seek to improve the mobility of the Li ion in order to achieve faster charge/discharge rates in Li-ion batteries.

Mehta et al.[27] cite a migration barrier for Li in Mo_2CS_2 equal to 0.22 eV. This difference with the results reported here has to do with the different structure reported for Mo_2CS_2–Li where Mehta et al. found that S sits on top of a C atom. This difference is a result of the different softwares used to perform DFT (VASP vs CASTEP), as well as the different pseudopotentials used. Still, if we were to accept that E_{bar} = 0.22 eV, $MoVCS_2$ exhibits 86.4% lower Li diffusion barrier. This reduction is also of high significance.

This result of E_{bar} = 0.03 eV we found here for $MoVCS_2$ is equal with the one found for the $Ti_3C_2Cl_2$ MXene in a previous study,[9] further reinforcing the use of MXenes as anode electrodes in Li-ion batteries.

Finally, in Figure 5, we see the calculated DOS for each structure. All materials are metallic (no bandgap at 0 eV, i.e., the Fermi level), a property that is essential for electrodes in Li-ion batteries.

CONCLUSIONS

Rechargeable ion batteries are energy storage devices whose operation is based predominantly on the intercalation of ions.[43] In general, an ion battery consists of a cathode (positive electrode) and an anode (negative electrode) in contact with an electrolyte which contains ions. The two electrodes are separated by a microporous polymer membrane (separator) which stops the electrons from passing between them alongside the ions.[44]

During charging of an ion battery cell, ions leave the positive electrode and move through the electrolyte to the negative electrode. We have, therefore, a storage of energy to the anode. During discharging of the battery, this energy is released, powering the battery, and the ions move back to the cathode.

One of the most active research fields regarding Li-ion batteries is the increase of their rate performance in order to reduce charging time which is important to the electric vehicles' market.[45] The materials of the electrodes are crucial for the performance of Li-ion batteries, as they determine capacity, cell voltage, and cyclability.[44]

Anode materials are still predominantly carbon-based; however, these anodes have almost reached their theoretical

https://doi.org/10.1021/acsomega.3c02080
ACS Omega XXXX, XXX, XXX−XXX

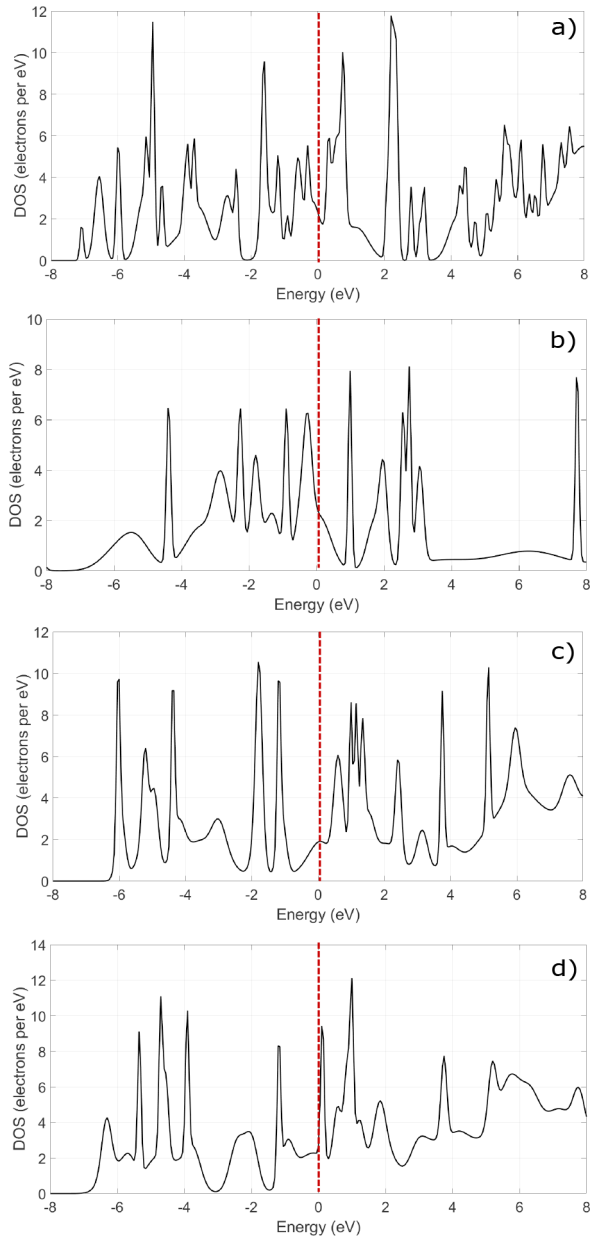

Figure 5. Calculated DOS for (a) Mo_2CS_2, (b) Mo_2CS_2−Li, (c) $MoVCS_2$, (d) $MoVCS_2$−Li. The Fermi level is shifted at 0 eV (red dashed line).

maximum capacity (372 $mAhg^{-1}$[44]). For this reason, carbon alternatives are being sought, with a particular focus on MXenes. A schematic of the working cycle of an ion battery, including an $MoVCS_2$ MXene anode, for example, can be seen in Figure 6.

In the present study, we examined the use of the Mo_2CS_2 MXene as an anode material for Li-ion batteries, where the upper layer of Mo atoms has been substituted by V. We found that this substitution renders the initial Mo_2CS_2 more thermodynamically stable, although experimental work has not yet been applied in depth to the kind of materials like the $MoVCS_2$ MXene. Furthermore, the substitution of the entire top Mo layer with V was shown to improve the mobility of the Li ion by 95%, while the material retains its metallic character. This fact makes the $MoVCS_2$ material a promising candidate

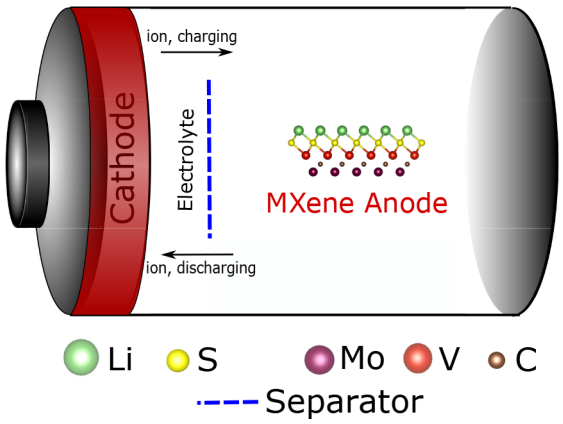

Figure 6. Inner workings of an ion battery with a $MoVCS_2$ MXene anode.

for the negative electrode in Li-ion batteries since it allows for faster charge/discharge rates than the Mo_2CS_2 MXene.

AUTHOR INFORMATION

Corresponding Author

Stavros-Richard G. Christopoulos − *Department of Computer Science, School of Computing and Engineering, University of Huddersfield, Huddersfield HD4 6DJ, U.K.; Centre for Computational Science and Mathematical Modelling, Coventry University, Coventry CV1 2TU, U.K.;* orcid.org/0000-0002-8468-2998; Email: S.R.Christopoulos@hud.ac.uk

Author

Konstantina A. Papadopoulou − *Department of Physics and Astronomy, Faculty of Environment, Science and Economy, University of Exeter, Exeter EX4 4QL, U.K.; Faculty of Engineering, Environment and Computing, Coventry University, Coventry CV1 5FB, U.K.;* orcid.org/0000-0002-8459-1201

Complete contact information is available at: https://pubs.acs.org/10.1021/acsomega.3c02080

Author Contributions

Konstantina A. Papadopoulou: Conceptualization, Methodology, Validation, Formal Analysis, Investigation, Resources, Data Curation, Writing-Original Draft, Visualization. Stavros-Richard G. Christopoulos: Conceptualization, Methodology, Validation, Resources, Data Curation, Formal Analysis, Writing-Review and Editing, Supervision, Project Administration, Funding Acquisition.

Notes

The authors declare no competing financial interest.

ACKNOWLEDGMENTS

The authors acknowledge support from the International Consortium of Nanotechnologies (ICON) funded by Lloyd's Register Foundation, a charitable foundation which helps to protect life and property by supporting engineering-related education, public engagement and the application of research.

REFERENCES

(1) Naguib, M.; Gogotsi, Y. Synthesis of two-dimensional materials by selective extraction. *Acc. Chem. Res.* **2015**, *48*, 128−135.

https://doi.org/10.1021/acsomega.3c02080
ACS Omega XXXX, XXX, XXX−XXX

(2) Verger, L.; Natu, V.; Carey, M.; Barsoum, M. W. MXenes: An Introduction of Their Synthesis, Select Properties, and Applications. *Trends in Chemistry* **2019**, *1*, 656.
(3) Hart, J. L.; Hantanasirisakul, K.; Lang, A. C.; Anasori, B.; Pinto, D.; Pivak, Y.; van Omme, J. T.; May, S. J.; Gogotsi, Y.; Taheri, M. L. Control of MXenes' electronic properties through termination and intercalation. *Nat. Commun.* **2019**, *10*, 1−10.
(4) Papadopoulou, K. A.; Chroneos, A.; Parfitt, D.; Christopoulos, S.-R. G. A perspective on MXenes: Their synthesis, properties, and recent applications. *J. Appl. Phys.* **2020**, *128*, 170902.
(5) Papadopoulou, K. A.; Chroneos, A.; Christopoulos, S.-R. G. Ion incorporation on the Zr2CS2MXene monolayer towards better-performing rechargeable ion batteries. *J. Alloys Compd.* **2022**, *922*, 166240.
(6) Barsoum, M. W.; El-Raghy, T. The MAX phases: Unique new carbide and nitride materials. *American Scientist* **2001**, *89*, 334−343.
(7) Sun, Z. Progress in research and development on MAX phases: a family of layered ternary compounds. *International Materials Reviews* **2011**, *56*, 143−166.
(8) Radovic, M.; Barsoum, M. W. MAX phases: bridging the gap between metals and ceramics. *American Ceramics Society Bulletin* **2013**, *92*, 20−27.
(9) Papadopoulou, K. A.; Parfitt, D.; Chroneos, A.; Christopoulos, S.-R. G. Behavior of Li-ion on the surface of Ti3C2−T (T= O, S, Se, F, Cl, Br) MXene: Diffusion barrier and conductive pathways. *J. Appl. Phys.* **2021**, *130*, 095101.
(10) Enyashin, A. N.; Ivanovskii, A. L. Structural and electronic properties and stability of MX enes Ti2C and Ti3C2 functionalized by methoxy groups. *J. Phys. Chem. C* **2013**, *117*, 13637−13643.
(11) Prolongo, S.; Moriche, R.; Jiménez-Suárez, A.; Sánchez, M.; Ureña, A. Advantages and disadvantages of the addition of graphene nanoplatelets to epoxy resins. *Eur. Polym. J.* **2014**, *61*, 206−214.
(12) Borysiuk, V. N.; Mochalin, V. N.; Gogotsi, Y. Molecular dynamic study of the mechanical properties of two-dimensional titanium carbides Tin+ 1Cn (MXenes). *Nanotechnology* **2015**, *26*, 265705.
(13) Yu, X.-f.; Cheng, J.-b.; Liu, Z.-b.; Li, Q.-z.; Li, W.-z.; Yang, X.; Xiao, B. The band gap modulation of monolayer Ti 2 CO 2 by strain. *RSC Adv.* **2015**, *5*, 30438−30444.
(14) Wang, H.; Wu, Y.; Zhang, J.; Li, G.; Huang, H.; Zhang, X.; Jiang, Q. Enhancement of the electrical properties of MXene Ti3C2 nanosheets by post-treatments of alkalization and calcination. *Mater. Lett.* **2015**, *160*, 537−540.
(15) Anasori, B.; Xie, Y.; Beidaghi, M.; Lu, J.; Hosler, B. C.; Hultman, L.; Kent, P. R.; Gogotsi, Y.; Barsoum, M. W. Two-dimensional, ordered, double transition metals carbides (MXenes). *ACS Nano* **2015**, *9*, 9507−9516.
(16) Anasori, B.; Shi, C.; Moon, E. J.; Xie, Y.; Voigt, C. A.; Kent, P. R.; May, S. J.; Billinge, S. J.; Barsoum, M. W.; Gogotsi, Y. Control of electronic properties of 2D carbides (MXenes) by manipulating their transition metal layers. *Nanoscale Horizons* **2016**, *1*, 227−234.
(17) Bai, Y.; Zhou, K.; Srikanth, N.; Pang, J. H.; He, X.; Wang, R. Dependence of elastic and optical properties on surface terminated groups in two-dimensional MXene monolayers: a first-principles study. *RSC Adv.* **2016**, *6*, 35731−35739.
(18) Naguib, M.; Kurtoglu, M.; Presser, V.; Lu, J.; Niu, J.; Heon, M.; Hultman, L.; Gogotsi, Y.; Barsoum, M. W. Two-dimensional nanocrystals produced by exfoliation of Ti3AlC2. *Adv. Mater.* **2011**, *23*, 4248−4253.
(19) Khazaei, M.; Arai, M.; Sasaki, T.; Chung, C.-Y.; Venkataramanan, N. S.; Estili, M.; Sakka, Y.; Kawazoe, Y. Novel electronic and magnetic properties of two-dimensional transition metal carbides and nitrides. *Adv. Funct. Mater.* **2013**, *23*, 2185−2192.
(20) Zhou, J.; Zha, X.; Chen, F. Y.; Ye, Q.; Eklund, P.; Du, S.; Huang, Q. A two-dimensional zirconium carbide by selective etching of Al3C3 from nanolaminated Zr3Al3C5. *Angew. Chem., Int. Ed.* **2016**, *55*, 5008−5013.
(21) Wang, C.-Y.; Guo, Y.-L.; Zhao, Y.-Y.; Zeng, G.-L.; Zhang, W.; Ren, C.-L.; Han, H.; Huai, P. A first-principles study on the vibrational and electronic properties of Zr-C MXenes. *Commun. Theor. Phys.* **2018**, *69*, 336.
(22) Champagne, A.; Charlier, J.-C. Physical properties of 2D MXenes: from a theoretical perspective. *Journal of Physics: Materials* **2021**, *3*, 032006.
(23) Meshkian, R.; Näslund, L.-Å.; Halim, J.; Lu, J.; Barsoum, M. W.; Rosen, J. Synthesis of two-dimensional molybdenum carbide, Mo2C, from the gallium based atomic laminate Mo2Ga2C. *Scripta Materialia* **2015**, *108*, 147−150.
(24) Sun, Q.; Dai, Y.; Ma, Y.; Jing, T.; Wei, W.; Huang, B. Ab initio prediction and characterization of Mo2C monolayer as anodes for lithium-ion and sodium-ion batteries. *journal of physical chemistry letters* **2016**, *7*, 937−943.
(25) Çakır, D.; Sevik, C.; Gülseren, O.; Peeters, F. M. Mo 2 C as a high capacity anode material: A first-principles study. *Journal of Materials Chemistry A* **2016**, *4*, 6029−6035.
(26) Mehta, V.; Tankeshwar, K.; Saini, H. S. Li-adsorption on doped Mo2C monolayer: A novel electrode material for Li-ion batteries. *AIP Conf. Proc.* **2018**, 140047.
(27) Mehta, V.; Saini, H. S.; Srivastava, S.; Kashyap, M. K.; Tankeshwar, K. S-functionalized Mo2C monolayer as a novel electrode material in Li-ion batteries. *J. Phys. Chem. C* **2019**, *123*, 25052−25060.
(28) Zhu, J.; Chroneos, A.; Eppinger, J.; Schwingenschlögl, U. S-functionalized MXenes as electrode materials for Li-ion batteries. *Applied Materials Today* **2016**, *5*, 19−24.
(29) Papadopoulou, K. A.; Chroneos, A.; Christopoulos, S.-R. G. Li-diffusion pathways in Zr2CO2 and Zr2CS2MXenes using the Bond Valence Sum model. *Comput. Mater. Sci.* **2022**, *201*, 110868.
(30) Jain, A.; Ong, S. P.; Hautier, G.; Chen, W.; Richards, W. D.; Dacek, S.; Cholia, S.; Gunter, D.; Skinner, D.; Ceder, G. Commentary: The Materials Project: A materials genome approach to accelerating materials innovation. *APL Materials* **2013**, *1*, 011002.
(31) Clark, S. J.; Segall, M. D.; Pickard, C. J.; Hasnip, P. J.; Probert, M. I.; Refson, K.; Payne, M. C. First principles methods using CASTEP. *Zeitschrift für Kristallographie-Crystalline Materials* **2005**, *220*, 567−570.
(32) Hohenberg, P.; Kohn, W. Inhomogeneous electron gas. *Phys. Rev.* **1964**, *136*, B864−B871.
(33) Kohn, W.; Sham, L. J. Self-consistent equations including exchange and correlation effects. *Phys. Rev.* **1965**, *140*, A1133−A1138.
(34) Payne, M. C.; Teter, M. P.; Allan, D. C.; Arias, T.; Joannopoulos, J. D. Iterative minimization techniques for ab initio total-energy calculations - molecular-dynamics and conjugate gradients. *Rev. Mod. Phys.* **1992**, *64*, 1045−1097.
(35) Pfrommer, B. G.; Cote, M.; Louie, S. G.; Cohen, M. L. Relaxation of crystals with the quasi-Newton method. *J. Comput. Phys.* **1997**, *131*, 233−240.
(36) Vanderbilt, D. Soft self-consistent pseudopotentials in a generalized eigenvalue formalism. *Phys. Rev. B* **1990**, *41*, 7892.
(37) Wan, W.; Wang, H. First-principles investigation of adsorption and diffusion of ions on pristine, defective and B-doped graphene. *Materials* **2015**, *8*, 6163−6178.
(38) Packwood, D.; Kermode, J.; Mones, L.; Bernstein, N.; Woolley, J.; Gould, N.; Ortner, C.; Csányi, G. A universal preconditioner for simulating condensed phase materials. *J. Chem. Phys.* **2016**, *144*, 164109.
(39) Brown, I. D. Recent developments in the methods and applications of the bond valence model. *Chem. Rev.* **2009**, *109*, 6858−6919.
(40) Chen, H.; Adams, S. Bond softness sensitive bond-valence parameters for crystal structure plausibility tests. *IUCrJ.* **2017**, *4*, 614−625.
(41) Govind, N.; Petersen, M.; Fitzgerald, G.; King-Smith, D.; Andzelm, J. A generalized synchronous transit method for transition state location. *Comput. Mater. Sci.* **2003**, *28*, 250−258.
(42) Morris, A. J.; Nicholls, R. J.; Pickard, C. J.; Yates, J. R. *OptaDoS user guide*; University of Cambridge, 2015.
(43) Liao, C. *Batteries*; IOP Publishing, 2021; pp 1-1−1−24.

https://doi.org/10.1021/acsomega.3c02080
ACS Omega XXXX, XXX, XXX−XXX

(44) Deng, D. Li-ion batteries: basics, progress, and challenges. *Energy Science & Engineering* **2015**, *3*, 385−418.
(45) Kang, B.; Ceder, G. Battery materials for ultrafast charging and discharging. *Nature* **2009**, *458*, 190−193.

https://doi.org/10.1021/acsomega.3c02080
ACS Omega XXXX, XXX, XXX−XXX